Acta Cryst. (1972). A**28**, 16.

Comparison of Experimental and *n*-Beam Calculated Intensities for Glancing Incidence High-Energy Electron Diffraction*

BY R. COLELLA† AND J. F. MENADUE‡

Departments of Materials Science and Engineering and of Applied Physics, Cornell University, Ithaca, New York 14850, *U.S.A.*

(*Received* 9 *October* 1970)

Rocking curves for the 2nd to 7th order reflections of the systematic set from the (111) planes of a highly perfect silicon single crystal have been obtained in an ultra-high-vacuum reflection electron diffraction camera operated at 40 keV. These have been compared with the profiles computed with an *n*-beam dynamic high-energy electron diffraction theory adapted to the Bragg case at glancing incidence. It is shown that, for the 333 reflection, six nodes of the *hhh* row from $\bar{1}\bar{1}\bar{1}$ up to 444 are adequate to take into account the systematic multiple beam interference effects. The calculated widths are found to agree with the observed widths within the experimental error for all reflections. The peak reflectivities computed initially for a perfect semi-infinite crystal are systematically higher than the experimental values, by a factor of 7 for the 222 node, decreasing to near agreement for the 777 node. Possible reasons for such discrepancies are discussed. Neither inelastic scattering effects nor reasonable changes in the silicon lattice potential near the surface can bring the observed and calculated intensities into agreement. The discrepancy can be considerably reduced for all orders of reflection, however, when the non-flat nature of the surface is considered.

1. Introduction

When electron diffraction from single crystals was discovered (Davisson & Germer, 1927), it was immediately understood that it could be used as a powerful tool for surface investigations. A considerable amount of work along this line was performed in the first few years subsequent to the original discovery (Pinsker, 1953) which showed the great complexity inherent in the problem. Since then, little progress was made in this field until recently, when ultra-high-vacuum techniques became available on a standard basis, and large and fast computers could be used for practical applications of the theory. We will be concerned in this paper with the Bragg case of electron diffraction at high energy ($E \simeq 40$ keV), which is expected to give information about the potential distribution and hence the charge density near the surface. The use of high-energy electron diffraction (HEED) should simplify the theoretical approach, in the sense that the scattering process can be considered as kinematical within the crystal unit cell (Colella, 1971).

In the recent literature of the Japanese school some quantitative applications of the *n*-beam dynamical theory in reflection were performed in order to explain some peculiar experimental facts. The breakdown of Friedel's law in multi-beam electron diffraction was quantitatively studied by Kohra (1954) who computed reflectivities *vs.* angle of incidence in three-beam cases, showing that the asymmetries experimentally observed in the diffraction patterns could be qualitatively explained by an *n*-beam dynamical treatment without introducing anomalous dispersion. The anomalous intensity of the specular beam at the crossing of a Kikuchi line has been extensively investigated by Miyake, Kohra & Takagi (1954), who performed *n*-beam computations of reflectivity *vs.* angle, under the assumption of zero absorption. In this way they could show how this anomalous enhancement was produced by multiple beam interactions. A subsequent work by Kohra, Molière, Nakano & Ariyama (1962) showed more accurate quantitative results, obtained by means of an electronic computer. These computations, in which absorption was apparently not taken into account, showed that the reflectivity of the specular beam could reach considerable peak values, 0·52 and 0·96 for two different angles of incidence. These aforementioned *n*-beam computations, however, were used to justify in a qualitative fashion some particular experimental facts. No real quantitative comparison between calculated and experimental Bragg reflection profiles has ever been presented.

More recently an ultra-high-vacuum, high-resolution electron diffraction camera was developed by Siegel & Menadue (1967), who have pointed out some possible advantages of using HEED rather than LEED for surface studies. It seems worthwhile at this stage to investigate the possibility of relating intensities to structure

* This work was supported by a grant from the Air Force Office of Scientific Research (Grant AF-AFOSR-1652-69). Partial support from the Advanced Research Projects Administration is also acknowledged.

† Present address: Department of Physics, Purdue University, Lafayette, Indiana 47907, U.S.A.

‡ Present address: Fritz-Haber-Institut der Max-Planck-Gesellschaft, Berlin-Dahlem, Germany.

factors in reflection of high-energy electrons, paralleling recent work in transmission experiments (Cowley, 1969).

The temperature dependence of the diffracted intensities can give information on the surface vibrational amplitudes which are complementary to those currently obtained at low energy.

The purpose of this paper is to compare the experimental results of Menadue (1972) with the application of the general theory to the Bragg case formulated by Colella (1972). A comparison of these measured values with theory for the systematic 111 reflections of silicon single crystal will be presented in this paper.

2. Experimental details

The experimental data (Menadue, 1972) were obtained from the (111) surface of nearly perfect silicon single-crystal specimens, all cut from an initial stock rod of *n*-type intrinsic material with a resistivity of 200 ohm. cm, and a dislocation density of <100 cm^{-2}.

The surfaces were polished to within $\pm 0{\cdot}1°$ of the (111) plane, and were cleaned by heating in the ultra-high-vacuum environment. This method was adopted to preserve as far as possible the flatness of the final cleaned surface. The cleaning procedure has been discussed elsewhere (Menadue, 1972), together with the details of the diffraction camera.

The divergence of the incident beam normal to the specimen surface was restricted to $1{\cdot}4\times10^{-4}$ rad, so that it was always considerably less than the narrowest peaks observed. The beam-defining aperture which set the divergence also limited the beam height, so that the incident beam fell entirely onto the diffracting surface for angles of incidence greater than 0·3° on specimens with a diameter of 8 mm.

The intensities of the *hhh* systematic series of reflections from a (111) silicon single crystal surface have been measured by a method equivalent to the ω X-ray scan. The total intensity reflected in the neighborhood of the 2θ direction was recorded as a function of θ, the angle of incidence to the (111) surface.

For each Bragg reflection it was possible to choose azimuths at which interference from non-systematic simultaneous reflections was greatly minimized. In this way the number of interacting nodes was greatly reduced, with considerable decrease in computing time. The rocking curves as recorded were practically azimuth-independent, which greatly simplified the comparison with theory.

Since the intensities observed with the well known 7 structure present on the surface were indistinguishable within the experimental error from those observed with the clean structure,* both sets of data have been averaged to improve the accuracy of the final data which is given in Tables 1 and 2. The data used here were obtained from one of the Syton polished specimens discussed by Menadue (1972). For the 222, 333, 444, and 555 reflections, the peak widths were reproducible within $\pm 10\%$. The peak heights were reproducible at different azimuths within $\pm 20\%$ for a given specimen, and the final data averaged for the clean and 7-structured surfaces have an error of less than $\pm 10\%$. In the present work the aperture on the measuring Faraday cup was a slit, subtending $5{\cdot}2\times10^{-3}$ rad at the specimen normal to the surface, and $5{\cdot}2\times10^{-4}$ rad parallel to the surface. This aperture was large enough to include all of the intensity (elastic or inelastic) associated with the specular reflection in the neighborhood of a Bragg peak, without including the general background between the Bragg peaks.

Table 1. *Experimental and calculated widths for the hhh systematic reflexions of silicon*

The extinction distances for all reflections are also given along with the number of (111) *d* spacings.

Reflection	Width (mrad)		Extinction distance	
	Exp	Calc	(Å)	(111) Layers
222	4·26	–	3·3	1·1
333	1·86	1·71	7·1	2·3
444	1·00	1·03	11	3·5
555	0·66	0·65	16	5·1
777	0·60	0·44	23	7·4

Table 2. *Experimental and calculated peak reflectances for the hhh systematic reflections of silicon*

Two different values for the Debye parameter have been used in the calculations

Reflection	Peak reflectance $R_{max}\times10^2$			Ratio $R^{exp}_{max}/R^{calc}_{max}$
	Exp.	Calc $B=B_{bulk}$	Calc $B=1{\cdot}4B_{bulk}$	$B=1{\cdot}4B_{bulk}$
222	5·3	39·1	38·8	0·14
333	3·7	19·6	18·2	0·20
444	3·0	11·9	10·3	0·29
555	0·67	2·06	1·56	0·43
777	0·39	0·95	0·575	0·68

3. Comparison with theory

A series of calculations have been performed for the Si (111) surface. Only interactions with reciprocal-lattice nodes of the *hhh* type have been considered (systematic reflections). Owing to the rapid decrease of the electron scattering factor with $\sin\theta/\lambda$, only nodes close to a limited spherical cap on the Ewald sphere are important. By a suitable choice of the azimuth it is possible, therefore, to avoid strong non-systematic interactions. The mean crystal potential V_0 has been assumed equal to 12 volts, as determined experimentally at 40 kV from the peak positions of the *hhh* systematics, averaged over different reflections (Menadue, 1972).

* A surface is referred to as a 'clean structure' in this text when its diffraction pattern in reflection is consistent with the bulk crystallographic structure.

The scattering factors, relativistically corrected for $E=40$ keV, have been computed using an analytical approximation (Doyle & Turner, 1968) for values of sin θ/λ higher than 0·35. Below this value this approximation is not believed to be valid, because it would lead at sin $\theta/\lambda=0$ to a mean crystal potential of 15·1 volts. The calculated f values, however, are based on a free atom model. Appreciable discrepancies with experiment are therefore to be expected at small values of sin θ/λ, which is the region where f is most sensitive to the charge distribution of the outer electrons (Raith, 1968; Anishchenko, 1966). For instance, Doyle & Turner (1968) show by calculation that the structure factor for the fundamental cell of NaCl is 20% smaller for ionized atoms with respect to neutral atoms, at sin $\theta/\lambda=0$. The f values for sin θ/λ between 0 and 0·35 have been interpolated so that $f(0)=4{\cdot}98$ Å (corresponding to $V_0=12$ volts).

Inelastic scattering effects are introduced by means of a complex potential (Yoshioka, 1957). Humphreys & Hirsch (1968) have calculated the ratio V'_g/V_g (imaginary to real part of the structure factors) as a function of g (magnitude of the scattering vector), for various elements. Their plots of V'_g/V_g neglect, however, single electron and plasmon excitations which are appreciable at small angle. There is some evidence (Meyer, 1966) that plasmon excitation is responsible for 60% of V'_0 in silicon, whereas only 12% is due to thermal diffuse scattering. This thermal contribution increases up to approximately 50% for higher order V'_g's. In view of these uncertainties, for the sake of simplicity, we preferred as a first approximation to set $V'_g/V_g=0{\cdot}1$, which has given satisfactory results for the interpretation of experimental micrographs (Hashimoto, Howie & Whelan, 1962). The effect of thermal vibrations has been introduced by multiplying each structure factor V_{H_j} by its appropriate temperature factor $\exp(-M_{H_j})$ (Ohtsuki, 1966) where $M_{H_j}=B(1/2d_{H_j})^2$, B is the Debye parameter, and d_{H_j} is the lattice spacing for the H_j planes.

The Debye parameter B was evaluated by fitting the n-beam calculated temperature dependence for the (333) and (777) with that experimentally determined. It turned out approximately $B=1{\cdot}4\ B_{\text{bulk}}$ where B_{bulk} is the Debye parameter consistent with the bulk Debye temperature $\theta_m=543\,°K$ (Batterman & Chipman, 1962).

The higher value of B, which implies larger vibration amplitudes for surface atoms, is not inconsistent with current experimental evidence (*e.g.* Morabito, Steiger & Somorjai, 1969). A detailed discussion of these data will be given in Batterman, Colella & Menadue (1971).

The boundary conditions for the continuity of the wave function on the crystal surface give suitable expressions for the amplitudes of the vacuum Bragg-diffracted waves

$$X_{H_j}=\sum_i C^i_{H_j}\psi^i \qquad (1)$$

where $i=1,2,\ldots n$ denotes the eigenvalues with positive imaginary part, C^i_H is the amplitude of a plane wave whose wave-vector is $\boldsymbol{\beta}^i_{H_j}$ and ψ^j is the amplitude of the ith Bloch wave. When the slice procedure is adopted i takes on the values 1,2, ... $2n$ (Colella, 1972).

We are considering only systematic reflexions in the symmetric case. Therefore the vacuum diffracted waves have all the same tangential component, which means that they are all coincident (in fact $\mathbf{k}^{\text{tang}}_{H_j}=\mathbf{k}^{\text{tang}}_0$ because $\mathbf{B}^{\text{tang}}_{H_j}=0$) along with the specular beam. The total diffracted intensity is therefore given (at any angle of incidence) by

$$I_{\text{vac}}=|\textstyle\sum_{H_j} X_{H_j}+R_0|^2 \qquad (2)$$

where the sum over H_j includes all the systematics (except the origin, related to R_0) and R_0 is the amplitude of the specular beam.

$$R_0=1-\textstyle\sum_i C^i_0\,\psi^i\,.$$

Fig. 1 shows the results of such a calculation for the 333, when two (000, 333) and six beams ($\overline{111}$ up to 444) are considered. A calculation performed with 8 beams (*i.e.* including $\overline{222}$ and 555) did not exhibit any appreciable difference from the 6-beam case. This means that the 333 computed profile is not appreciably sensitive to the excitation of nodes other than those between the origin and the 333 plus the two adjacent ones, $\overline{111}$ and 444. The criterion of neglecting further nodes will be even more valid for higher

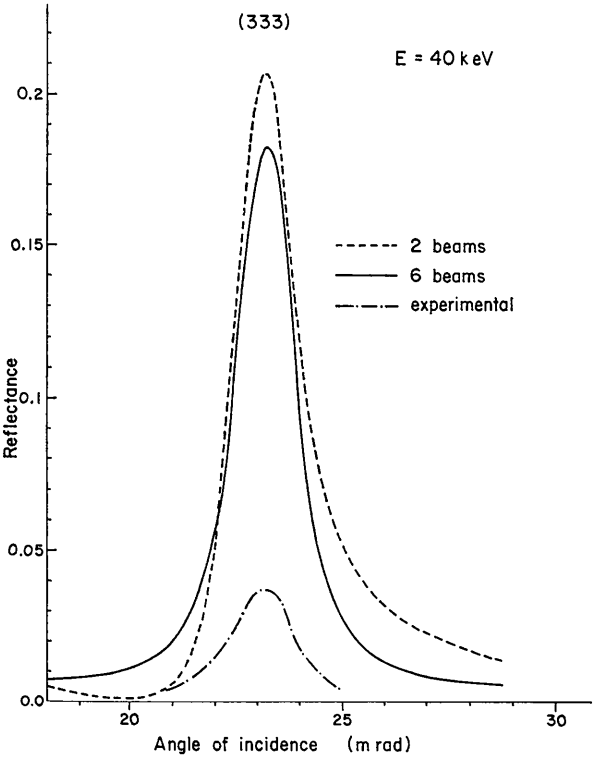

Fig. 1. Comparison of observed 333 reflection with 2-beam and 6-beam calculations. $E=40$ keV, $V_0=12$ volts.

orders because (i) the distance between the Ewald sphere and the closest neglected nodes increases with $\sin\theta/\lambda$, and (ii) the structure factors V_{hhh} decrease rapidly with $\sin\theta/\lambda$. The same calculation was performed for other systematics, 444, 555, and 777.* The nodes considered for the *n*-beam calculation, in each case, were those between $\overline{111}$ and $h+1$, $h+1$, $h+1$ for the *hhh* reflection. Therefore the number of beams involved was seven, eight and ten respectively. The main features of these computed profiles, namely: peak intensity and full width at half height, are tabulated in Tables 1 and 2 along with the corresponding experimental values. These can be obtained directly from the recorded profiles of the rocking curves, which are practically unaffected by the divergence of the incident beam of $1{\cdot}4\times10^{-4}$ radians.

4. Discussion

It is apparent from Fig. 1 that the *n*-beam effects are not very important for the 333 reflection.† When comparing profiles, there is a marked discrepancy between theoretical and experimental peak reflectivities, whereas the widths are in agreement. The same general features are exhibited by other *hhh* reflections. For all reflections considered the calculated two-beam widths are changed very little by the inclusion of other systematic reflections. A more detailed discussion is given below.

(*a*) *Widths*

The observed and calculated full widths at half height are presented in Table 1, with consistent agreement within experimental error for all orders of reflection. The agreement supports the value of 0·1 used for V_g'/V_g in the calculation. Higher values for this ratio would result in calculated widths exceeding the observed widths, so that an upper limit of 0·1 could have been determined by matching the widths.

The computed width for the 222 does not appear in Table 1. It could not be evaluated from the computed profile because of the rapidly rising background due to the specular beam on the low-angle side. Such a strong low-angle background was much weaker in the experimental profile, probably owing to surface non-flatness.

The refractive deviation of the beam in passing through a (111) surface plane was in general considerably greater than either the half width of the Bragg reflection peak or the divergence angle of the incident beam. If a significant portion of the beam enters or leaves through non-(111) surfaces, each Bragg reflection may be smeared, or may appear at more than one angle of incidence. For the present studies the observed and calculated peak widths are in good agreement up to the 777 reflection. Also the Bragg peaks occur at refractively shifted positions corresponding to a constant mean inner potential. These observations are consistent with the beam passing through a surface closely parallel to the (111) planes. If some kind of surface non-flatness is allowed for, the undulations would then consist of (111) facets joined by steps. When the topmost blocks are sufficiently short in the direction of the beam so that they can be penetrated ($\sim$100 Å), extra peaks would occur, with a negligible refractive shift. This effect has been observed in the case of surfaces with $\sqrt{19}$ structure (Menadue, 1971).

The extinction distances are also included in Table 1. These are the depths, measured normal to the surface, at which the total field intensity is reduced to $1/e$ of the initial value at the surface (see Appendix). It is seen that energy flow is confined to the top 2 or 3 layers for the lowest order reflections.

(*b*) *Peak heights*

The observed and calculated peak reflectances for room temperature are presented in Table 2.

The calculated values have been based for the initial data in column 3, on the bulk Debye temperature of 543 °K (Batterman & Chipman, 1962). It is to be expected that the mean-square amplitude of thermal vibration of the surface layer will be greater than that of the bulk, owing to the greater freedom of the atoms to move along the normal to the surface plane. It was found that using the bulk value of the Debye parameter B did in fact predict slopes for the peak reflectances as a function of temperature which were too shallow. For the purpose of the present calculations, a single compromise value of $1{\cdot}4B_{\text{bulk}}$ was used for all reflections justified only at this stage by the fact that it resulted in a temperature dependence for the 333 and 777 which were in agreement with the experiment. The peak reflectances using this Debye parameter are given in column 4 of Table 2, and the ratios of experimental to calculated peak intensities are taken in column 5. The experimental values are considerably less than the calculated, the discrepancy becoming less for the higher order reflections.

We will consider in the following discussion some possible reasons for such discrepancies.

Inelastic scattering has already been discussed in § 3. A value of V_g'/V_g of 0·2 was tried for the 333 reflection, to allow for increased inelastic scattering. The peak height was reduced by a factor 2·9, but the width increased by a factor 1·5 exceeding the experimental value. Thus it does not seem possible that the ratio V_g'/V_o' can be higher than 0·1, which is also supported by experimental measurements of V_g' and V_o' by Meyer (1966) and Kreutle & Meyer-Ehmsen (1969).

The size of the aperture on the Faraday cup (§ 2) was such that when a rocking curve was recorded the con-

* The 666 was avoided because it is a forbidden reflection and its experimental intensity is strongly azimuth-dependent. The assumption that only systematic interactions are important is no longer valid.

† This statement is not valid in general. For instance, in the case of tungsten, the two-beam profiles are appreciably different from *n*-beam computations (unpublished).

tribution of the associated Kikuchi line was included throughout the profile. It is not clear at this stage how important this inelastic contribution is when the experimental profiles are compared with computations in which only elastic scattering is taken into account. If the contribution of the Kikuchi line was important, however, the comparison between experiment and theory would be further worsened.

The effect of modifying the bulk potential near the surface was tested, for the 333 and for the 444 reflections. There is experimental evidence (Pinsker, 1953) that the average inner potential V_0 decreases near the surface. The rocking curves were recomputed, assuming on a purely empirical basis that V_0 undergoes a decrement of 40% near the surface, and that the V_{H_j}'s were similarly affected. Changes in lattice spacing were not considered, since their effect on the diffraction profiles was found to be negligible (Colella, 1972, § 5).

This calculation was performed for the 333 and 444 reflections, with two slices in each case, whose thicknesses were arbitrarily set equal to 3 Å. Six and seven beams were taken into account, respectively, as in the case of the uniform crystal model (§ 3). An exponential decay for $V_{H_j}^{\text{surf}}$ to $V_{H_j}^{\text{bulk}}$ was assumed, such that in the first slice, on top of the bulk, the correcting factor for the Fourier components of the potential was assumed equal to the square root of the corresponding correcting factor in the second slice. These modifications resulted in peak positions, widths at half height, and, for the 444, a peak reflectivity which were practically unchanged from the semi-infinite crystal model calculations. The major effect was to reduce the 333-peak reflectance by 14%. If the thickness of each slice is increased to 6 Å, the peak reflectances are further decreased to values which are still much higher than the experimental values, and the widths are considerably increased, contrary to the observations. As the surface potential is further decreased, there is a tendency for a shift of the diffraction peaks to the high-angle side. It does not seem at all likely that the main part of the discrepancy could be due to modifications of the bulk silicon potentials.

It is not unreasonable to assume that surfaces which have been heated to temperatures at which the bulk material has evaporated at a significant rate (as in the present cleaning procedure) have an undulating nature. Diffraction conditions are then of the quasi-reflection kind mentioned by Tompsett & Grigson (1966). When the average length of the undulations becomes larger than the extinction distances, and the maximum angle of the steepest part of the undulations exceeds the angle of incidence, a considerable proportion of the reflected beam will be lost by being unable to penetrate the effectively opaque side of the undulation above it, as shown in Fig. 2(*a*).

For the purpose of calculation a very simple model of the undulations was considered. It was assumed that the undulations had variable amplitude A and wavelength L, and that these were related by a consistent maximum slope $\alpha = \pi A/L$, as for a sinusoidal waveform. The single parameter α then determines the proportion of reflected intensity which is lost for a given vacuum angle of incidence to the net reflecting planes, θ_0. In Fig. 2(*a*) it is seen that reflected beams generated between a and b will be masked by the rise of the undulation above, while those generated between b and c, the tangent points for the particular angle of incidence (and therefore of reflection), will contribute to the observed diffraction peak. The proportion of observed intensity to total reflected intensity is thus $p = (t+s)/t$, where t and s are defined in Fig. 2(*a*). Fig. 2(*a*) was drawn for a particular angle of incidence $\theta_0 = \beta$, at which angle the incident beam tangent at c just reaches a, the lowest point on the undulation. From this point the reflected beam is just tangent again at b. For higher angles of incidence, beams incident in the neighborhood of a can also reflect to the detector, as in Fig. 2(*b*). For $0 < \theta_0 < \beta$, the greater part of the range of interest, this model predicts that the proportion of detected intensity will be $p = (1/\pi) \arcsin(\theta_0/\alpha)$.

Assuming that the non-flatness has had a major effect on the intensities, other effects as discussed above were neglected and the proportion p was taken as being equal to the ratio of observed to calculated peak reflectance, from Table 2.

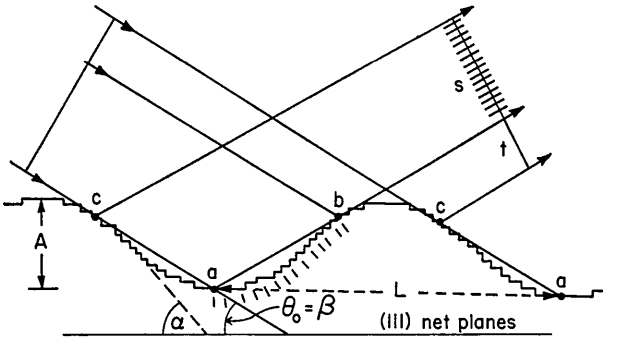

(*a*)

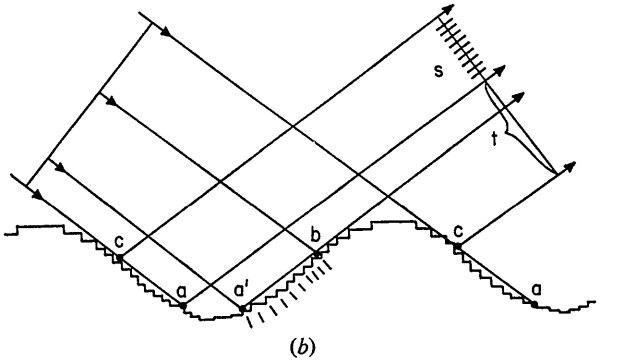

(*b*)

Fig. 2. Surface undulation model. The t beam reaches the detector, but the s beam is shaded out by the rising undulation (cross-hatched area). (*a*) is drawn for a particular angle of incidence $\theta_0 = \beta$ such that the incident beam just reaches a, the lowest point on the undulation. (*b*) is for $\beta < \theta_0 < \alpha$.

It should be observed that this correction does not act appreciably on the peak widths, since the correcting factor p is a smooth function of θ.

In Table 3 it is seen that α is sensibly constant within the expermental error for the 3rd-, 4th- and 5th- order reflections. The 777 data cannot be used with the above simple expression since the angle of incidence θ_0 exceeds the value of α calculated for the lower-order reflections. Because the penetration is so limited for the 222 reflection, the peak intensity data would be most sensitive to the structure of the surface monolayer. The value of α averaged over the 3rd-, 4th- and 5th- order reflections was 0·043 rad, or 2·5° which is not unreasonable. Even allowing for the extreme simplicity of the model used here, it is apparent that surface non-flatness can have a major effect on the observed intensities.

Table 3. *Proportion of detected intensity for the various orders of reflection*

The corresponding angles of incidence are also given along with the maximum slope of the sinusoidal profile.

Reflection	P	θ_0 (mrad)	α (mrad)	
222	0·14	0·0098	0·024	
333	0·20	0·0232	0·039	$\langle\alpha\rangle$ = 0·043 mrad
444	0·29	0·0346	0·042	= 2·5°
555	0·43	0·0451	0·047	
777	0·68	0·0654	–	

5. Conclusions

The rocking curve profiles which were obtained from the *hhh* systematic set of reflections from the (111) surface of silicon have been compared with profiles computed from the n-beam dynamical theory adapted to the Bragg case. The widths of the experimental profiles agree within experimental error with the n-beam calculations for all orders of reflection. The experimental peak intensities, however, are systematically lower than the calculated values, by a factor which ranges from 0·14 for the 222 up to 0·68 for the 777 reflections. It is apparent that the more penetrating reflections are in better agreement with the computations. Possible reasons for such discrepancies are inelastic scattering, modification of the crystal potential near the surface, and the effects of non-flatness of the surface. Within the limitations of the assumptions considered, it seems that changes of the surface potential within the first few layers do not appreciably affect the computed profiles. Results based on a very simple model, however, indicate that large effects on the observed intensities are possible due to departures from flatness, particularly for the lowest angles of incidence. It is concluded that the n-beam dynamical theory of high-energy electron diffraction, such as that developed for the transmission case, can be applied as a first approximation to the glancing incidence case with the appropriate boundary conditions. A major limitation in the applicability of the theory seems to lie in deviations from flatness.

The authors benefited from many enlightening and stimulating discussions with Professor B. W. Batterman, who read critically the manuscript. This work was made possible through a Grant from AFOSR (AF-1652-69) and was aided by the support facilities of the Materials Science Center at Cornell University.

APPENDIX

Calculation of the extinction length

The extinction length is defined here as the distance in the crystal, normal to the surface, at which the total wave-field intensity $|\psi|^2$, as defined in § 2 (equation 2) of Colella (1972), is reduced to $1/e$ with respect to its value at the surface. When the wave-field intensity is averaged over the crystal cell and the 'Pendellösung'* period, the following expression is obtained:

$$|\psi|^2 = \sum_1^n{}_p \exp(-4\pi\gamma_{0t}^p t)|\psi^p|^2 \sum_0^{Hm}{}_{H_j} |C_{Hj}^p|^2 \qquad \text{(A1)}$$

where $0, H_2, H_3 \ldots H_m$ are the excited nodes in reciprocal space, C_{Hj}^p is the amplitude of a plane wave having wave-vector $\boldsymbol{\beta}_{Hj}^p = \boldsymbol{\beta}_0^p + \mathbf{B}_{Hj}$, $\boldsymbol{\beta}_0^p$ is the pth eigen wave-vector inside the crystal for those plane waves whose wave-vectors have the same tangential component as the external incident beam $\mathbf{k}_0$, $\mathbf{B}_{Hj}$ is the reciprocal-lattice vector pertinent to the node H_j, ψ^p are the amplitudes of the Bloch waves, γ_{0t}^p is the imaginary part of the normal component of $\boldsymbol{\beta}_0^p$, t is the depth at which $|\psi|^2$ is evaluated. Only the eigenvalues whose imaginary parts are positive have been considered in (A1), as explained in § 4 of Colella (1971).

* Beating between different eigenvalues of the same wave-vector.

References

ANISHCHENKO, R. I. (1966). *Phys. stat. sol.* **18**, 923.

BATTERMAN, B. W. & CHIPMAN, D. R. (1962). *Phys. Rev.* **127**, 690.

BATTERMAN, B. W., COLELLA, R. & MENADUE, J. (1971). In preparation.

COLELLA, R. (1972). *Acta Cryst.* A**28**, 11.

COWLEY, J. M. (1969). *Acta Cryst.* A**25**, 129.

DAVISSON, C. J. & GERMER, L. H. (1927). *Phys. Rev.* **30**, 705.

DOYLE, P. A. & TURNER, P. S. (1968). *Acta Cryst.* A**24**, 390.

HASHIMOTO, H., HOWIE, A. & WHELAN, M. J. (1962). *Proc. Roy. Soc.* A**269**, 80.

HUMPHREYS, C. J. & HIRSCH, P. B. (1968). *Phil. Mag.* **18**, 115.

KOHRA, K., MOLIÈRE, K., NAKANO, S. & ARIYAMA, M. (1962). *J. Phys. Soc. Japan*, **17** Supplement B-II, 82.

KREUTLE, M. & MEYER-EHMSEN G. (1969). *Phys. stat. sol.* **35**, K17.
MENADUE, J. F. (1972). *Acta Cryst.* A**28**, 1.
MEYER, G. (1966). *Phys. Letters*, **20**, 240.
MIYAKE, S., KOHRA, K. & TAKAGI, M. (1954). *Acta Cryst.* **7**, 393.
MORABITO, J. M. JR, STEIGER, R. F. & SOMORJAI, G. A. (1969). *Phys. Rev.* **79**, 638.
OHTSUKI, Y. H. (1966). *J. Phys. Soc. Japan*, **21**, 2300.
PINSKER, Z. G. (1953). *Electron Diffraction*. London: Butterworths.
RAITH, H. (1968). *Acta Cryst.* A**24**, 85.
SIEGEL, B. M. & MENADUE, J. F. (1967). *Surface Sci.* **8**, 206.
TOMPSETT, M. F. & GRIGSON, C. W. B. (1966). *J. Sci. Instrum.* **43**, 430.
YOSHIOKA, H. (1957). *J. Phys. Soc. Japan*, **12**, 618.

Acta Cryst. (1972). A**28**, 22

The X-ray Debye Temperature of Aluminum

BY R. E. DINGLE* AND E. H. MEDLIN
Department of Physics, University of Adelaide, Adelaide 5001, *Australia*

(*Received* 30 *March* 1971)

Accurate photographic X-ray intensities have been obtained for nearly all reflexions within the Mo $K\alpha$ limiting sphere for two single crystals of aluminum. These intensities have been used to give the X-ray Debye temperature, Θ_D, in the first part of an experimental determination of the electron-density distribution in solid aluminum. The results of this work show that $\Theta_D = 393 \pm 1$ °K at 293 °K, varying with temperature to $\Theta_D = 362 \pm 9$ °K at 559 °K. The Debye parameter is found to be $0{\cdot}849 \pm 0{\cdot}005$ Å^2 at 293 °K.

Introduction

It is of course the electron distribution in an atom that is responsible for its physical and chemical properties. In the free atom it is relatively simple to calculate the electron wave functions, the electron distribution and the X-ray scattering factors, *f*. Agreement to 1% is obtained with absolute experimental results by Chipman & Jennings (1963) for X-ray scattering out to $s = \sin\theta/\lambda \simeq 0{\cdot}4$ by the spherically symmetrical monatomic gases neon, argon, krypton and xenon, but this is not so for some monatomic metallic solids where differences of *ca.* 4% have been found between experimental and Hartree–Fock free-atom scattering factors for low-angle reflexions by Batterman, Chipman & de Marco (1961) and subsequently by other workers as discussed by Weiss (1966). Free-atom wave functions cannot be, and are not, valid for the solid state; it is of interest to know in what way the free-atom wave functions are modified by solid-state interactions and we have asked this question for aluminum.

Accurate absolute measurements have been made on a number of X-ray reflexions from aluminum by a number of workers (Batterman *et al.*, 1961; Bensch, Witte & Wölfel, 1955; De Marco, 1967; Järvinen, Merisalo & Inkinen, 1969, Raccah & Henrich 1969, 1970; Inkinen, Pesonen & Paakkari 1970); their results confirm a solid-state effect and suggest that this is due to a redistribution of the conduction electrons alone. On the other hand, the enigma with aluminum is that, in order to account for the fact that the low-angle scattering factors are less than those calculated for the 10 neon-core electrons alone, an unlikely core electron redistribution is suggested (Weiss, 1966). In any case recent theoretical scattering factors obtained by Arlinghaus (1967) from solid-state wave functions based on augmented-plane-wave calculations of the 3*s*, 3*p* and indeed 2*p* energy bands have left the dilemma unresolved. The present position is that no solid-state wave functions have yet been obtained that can account for the low-angle scattering factors of aluminum.

Further, the limitation of diffraction data in reciprocal space leads to uncertainties in charge-distribution information. Present uncertainties are such as to justify its more accurate determination from a greater number of reflexion data and we have obtained these to $\sin\theta/\lambda \simeq 1{\cdot}4$ Å^{-1}. Other workers have been able to meet the required accuracy of *ca.* ±1% in atomic scattering factors and to make comparisons between calculated and observed values in spite of uncertainties in the Debye parameter, *B*, and the X-ray Debye temperature, Θ_D, which specify the effect of temperature on the intensities of X-rays scattered from a material. To make such comparisons, either the calculated scattering factors are to be multiplied by $\exp(-Bs^2)$ or the experimental values are to be multiplied by $\exp(Bs^2)$. With the small range of $\sin\theta/\lambda$ (*ca.* 0·6 Å^{-1}) for the first nine reflexions, any reasonable Debye temperature may be assumed. Raccah & Henrich (1969) chose $\Theta_D = 387$ °K but, with their limited range of data, little error would have resulted from the use

* Present address: Defence Standards Laboratories, Woodville North 5012, South Australia.